# Predicting motor improvement after stroke with clinical assessment and diffusion tensor imaging

*Ethan R. Buch*[a], *Sviatlana Rizk*[b], *Pierre Nicolo, Leonardo G. Cohen*[a], *Armin Schnider*[b], *Adrian G. Guggisberg*[b]

[a] Human Cortical Physiology Section, NINDS, NIH, Bethesda, USA
[b] Department of Clinical Neurosciences, University Hospital of Geneva, Geneva, Switzerland

**Appendix e-1 (Supplemental Methods)**

Patients

Patients gave written informed consent to participate in this study and all procedures were approved by the local ethics committee. Patients were diagnosed with first unilateral, ischemic stroke in the territories of the middle and/or anterior cerebral artery or unilateral hemorrhagic hemispheric stroke. Exclusion criteria were: previous neurological, psychiatric, or cognitive impairment; preexisting brain lesion visible in the CT/MRI on admission (except lacunar lesions or white matter hyperintensities); epileptic seizures; persistent post stroke delirium; ischemic lesions in the brain stem, or cerebellum; metallic objects in the brain or pacemaker; medical complications. All patients received standard therapy at the stroke unit during the acute phase and an individually tailored multidisciplinary rehabilitation program in the subacute and chronic phases.

Patients had a mean NIH Stroke Score of 11 (range 3 to 27), with twelve having right hemispheric lesions (Table e-1).

Diffusion tensor imaging

Whole brain, single-shot echo-planar (EPI) diffusion-weighted volumes (30 non-collinear directions; b=1000smm−2; 64 slices; voxel size 1.8 × 1.8 × 2.0 mm3; echo time/repetition time = 82 ms/8.2 s; acquisition time = 4 min 40 sec) plus one volume without diffusion weighting (b = 0 smm−2) were acquired parallel to a line intersecting the anterior and posterior commissure on a 3.0 Tesla Siemens Trio TIM 3.0T scanner using an 64-channel coil. High-resolution structural T2-weighted (echo time/repetition time = 376 ms/5.0 s; voxel size = 0.45 × 0.45 × 0.90 × mm3) volumes were also acquired.

Preprocessing of the diffusion weighted images was performed via the TORTOISE software package (https://science.nichd.nih.gov/confluence/display/nihpd/TORTOISE)[1]. Diffusion weighted images were first corrected for motion and eddy current distortions[2], including proper reorientation of the b-matrix to account for the rotational component of the subject rigid body motion[3]. In addition, B0 susceptibility-induced echo planar image distortions were corrected using an image registration-based approach using B-splines[4]. All corrections were performed in the native space of the diffusion-weighted images. A robust non-linear diffusion tensor model (RESTORE[5]) was then fit to the corrected data.

Following tensor estimation, nonlinear spatial registration to MNI-space was performed using a non-parametric, diffeomorphic deformable image registration technique implemented in DTI-TK (www.nitrc.org/projects/dtitk/), which incrementally estimates its displacement field using a tensor-based registration formulation[6]. It is designed to take advantage of similarity

measures comparing tensors as a whole via explicit optimization of tensor reorientation and includes appropriate reorientation of the tensors following deformation. The IIT human brain atlas (https://www.nitrc.org/projects/iit/) was used as the target for this spatial registration pipeline[7].

Fractional anisotropy (FA) maps were derived for each patient and skeletonized via thresholding at 0.2. They were then convolved with binarized masks for the right and left corticospinal tract (CST) included in the IIT human brain atlas. In order to reduce partial volume effects or small misalignments in the registration, the masks were further refined by only considering voxels that were found in at least 75% of the individual maps for the patient group. Mean FA values were then determined for both the ipsilesional and contralesional CST in each patient.

CST asymmetry was calculated from the mean fractional anisotropy (FA) of the CST[8]:

$(FA_{contralesional} - FA_{ipsilesional})/(FA_{contralesional} + FA_{ipsilesional})$.

Lesion size and location

T2-weighted three-dimensional fast spin-echo, DWI, and FLAIR sequences were used to delineate ischemic lesions in the software MRIcro (http://www.cabiatl.com/mricro/) written by Chris Rorden. Lesion maps are visualized in Figure e-1. Lesion size was defined as the ratio between lesion volume and the volume of the skull stripped brain extracted from co-registered T1 sequences. The primary motor cortex was defined as region of interest with the human motor area template[9] and the percentage affected by the lesion was computed.

Statistical Analyses

The association between CST asymmetry and clinical variables was assessed with Spearman correlations, since clinical variables were not normally distributed.

A logistic regression model with leave-one-out crossvalidation (LOC) was used to classify between recovery-typical and recovery-atypical patients. The significance of classification accuracy was assessed with a permutation test. In each of 5000 permutation loops, the order of CST asymmetry values was shuffled across patients and a new logistic regression model with LOC was computed. The significance of the prediction accuracy was estimated from its position in the empirical distribution obtained through permutations.

**Figure e-1**

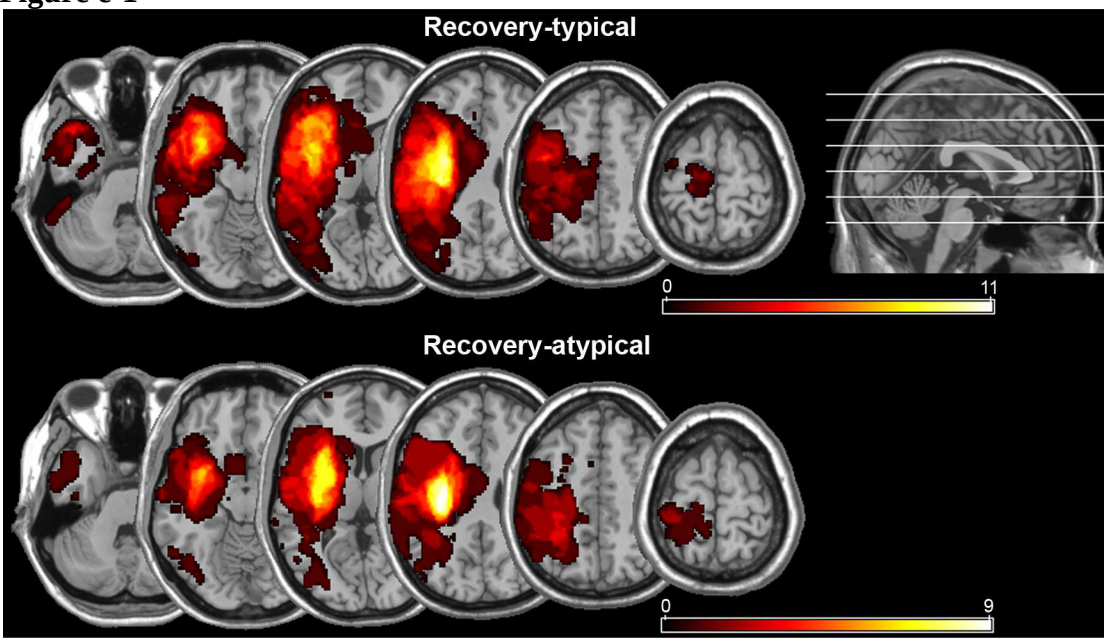


**Lesion maps of recovery-typical and atypical patients.** All lesions are aligned to the same hemisphere for visualization.

**Figure e-2**

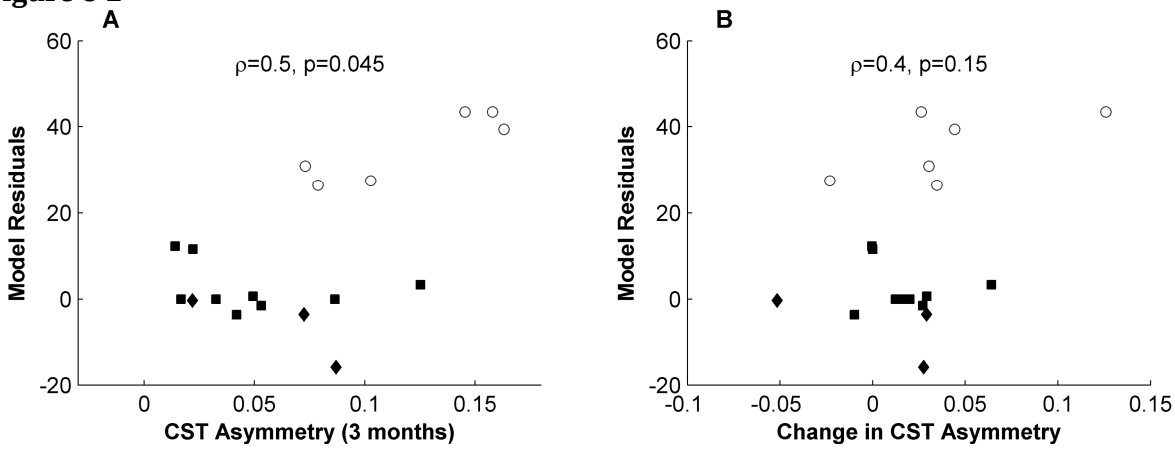


**DTI imaging at 3 months does not further improve prediction of recovery. (A)** As at 2 weeks, CST asymmetry at 3 months was predictive of atypical recovery, but the association did not become stronger. **(B)** The change in CST asymmetry from 2 weeks to 3 months after stroke was not significantly associated with model residuals. This suggests that initial CST affection is mainly responsible for atypical recovery.

**Table e-1. Patient characteristics.**

| Age | Gender | Lesion Side | Admission NIHSS | Handedness | Suspected Stroke Etiology |
|---|---|---|---|---|---|
| 67 | M | R | 13 | R | Internal carotid artery stenosis |
| 65 | M | L | 4 | L | Microangiopathic |
| 60 | M | L | 16 | R | Cryptogenic |
| 80 | F | R | 5 | R | Atrial fibrillation |
| 52 | F | R | 11 | R | Primary CNS vasculitis |
| 74 | F | L | 14 | R | Akinetic left ventricular segment |
| 48 | F | L | 27 | R | Cryptogenic |
| 54 | F | L | 6 | R | Patent foramen ovale |
| 62 | M | R | 9 | R | Internal carotid artery occlusion |
| 62 | M | L | 4 | R | Microangiopathic |
| 68 | M | R | 16 | R | Atrial fibrillation |
| 37 | M | L | 8 | R | Patent foramen ovale and DVT |
| 63 | M | L | 12 | R | Internal carotid artery occlusion |
| 70 | F | L | 14 | R | Atrial fibrillation |
| 53 | M | L | 20 | R | Internal carotid artery dissection |
| 46 | F | R | 4 | R | Cryptogenic |
| 78 | F | R | 9 | R | Atrial fibrillation |
| 81 | F | R | 6 | L | Cryptogenic |
| 53 | M | R | 5 | R | Internal carotid artery dissection |
| 47 | M | R | 3 | R | Cryptogenic |
| 67 | F | L | 11 | R | Atrial flutter and mitral valve |
| 43 | M | L | 18 | L | Patent foramen ovale and DVT |
| 52 | M | R | 14 | R | Middle cerebral artery stenosis |
| 49 | F | R | 16 | R | Cryptogenic |
| 83 | M | L | 14 | L | Microangiopathic |

## e-References


1. Pierpaoli C, Walker L, Irfanoglu MO, et al. TORTOISE: an integrated software package for processing of diffusion MRI data. ISMRM 18th Annual Meeting. Stockholm, Sweden2010.
2. Rohde GK, Barnett AS, Basser PJ, Pierpaoli C. Estimating intensity variance due to noise in registered images: applications to diffusion tensor MRI. Neuroimage 2005;26:673-684.
3. Leemans A, Jones DK. The B-matrix must be rotated when correcting for subject motion in DTI data. Magn Reson Med 2009;61:1336-1349.
4. Wu M, Chang LC, Walker L, et al. Comparison of EPI distortion correction methods in diffusion tensor MRI using a novel framework. Medical image computing and computer-assisted intervention : MICCAI International Conference on Medical Image Computing and Computer-Assisted Intervention 2008;11:321-329.
5. Chang LC, Jones DK, Pierpaoli C. RESTORE: robust estimation of tensors by outlier rejection. Magn Reson Med 2005;53:1088-1095.
6. Zhang H, Yushkevich PA, Alexander DC, Gee JC. Deformable registration of diffusion tensor MR images with explicit orientation optimization. Medical image analysis 2006;10:764-785.
7. Varentsova A, Zhang S, Arfanakis K. Development of a high angular resolution diffusion imaging human brain template. Neuroimage 2014;91:177-186.
8. Stinear CM, Barber PA, Smale PR, Coxon JP, Fleming MK, Byblow WD. Functional potential in chronic stroke patients depends on corticospinal tract integrity. Brain 2007;130:170-180.
9. Mayka MA, Corcos DM, Leurgans SE, Vaillancourt DE. Three-dimensional locations and boundaries of motor and premotor cortices as defined by functional brain imaging: a meta-analysis. Neuroimage 2006;31:1453-1474.